

## MIT Open Access Articles

### *Precise orbit and baseline determination for maneuvering low earth orbiters*

The MIT Faculty has made this article openly available. **Please share** how this access benefits you. Your story matters.

**Citation:** Ju, Bing et al. "Precise Orbit and Baseline Determination for Maneuvering Low Earth Orbiters." GPS Solutions (2015): n. pag.

**As Published:** <http://dx.doi.org/10.1007/s10291-015-0505-x>

**Publisher:** Springer Berlin Heidelberg


**Persistent URL:** <http://hdl.handle.net/1721.1/104780>

**Version:** Author's final manuscript: final author's manuscript post peer review, without publisher's formatting or copy editing

**Terms of use:** Creative Commons Attribution-Noncommercial-Share Alike



# Precise orbit and baseline determination for maneuvering low earth orbiters

Bing Ju<sup>1,2</sup>  · Defeng Gu<sup>1</sup> · Thomas A. Herring<sup>2</sup> · Gerardo Allende-Alba<sup>3</sup> · Oliver Montenbruck<sup>3</sup> · Zhengming Wang<sup>1</sup>

Received: 15 April 2015 / Accepted: 18 November 2015  
© Springer-Verlag Berlin Heidelberg 2015

**Abstract** Orbital maneuvers are usually performed as needed for low earth orbiters to maintain a predefined trajectory or formation-flying configuration. To avoid unexpected discontinuities and to connect pre- and post-maneuver arcs with a minimal set of parameters, a maneuver has to be considered in the routine GPS-based orbit determinations. We propose a maneuver handling method in a reduced-dynamic scheme. With the proper thrust modeling and numerical integration strategy, the effects caused by orbital maneuver can be largely eliminated. The performance for both single-satellite precise orbit determination (POD) and inter-satellite precise baseline determination (PBD) is demonstrated using selected data sets from the Gravity Recovery and Climate Experiment (GRACE) mission. For the POD results, the orbit determination residuals indicate that the orbit with maneuver modeling is well fit to the GPS observations. The external orbit validation shows that the GRACE-B orbits obtained from our approach match the DLR reference orbits better than 3 cm (3D RMS), which is comparable to the result of the maneuver-free GRACE-A satellite. For the PBD results, on average 87 % of double-difference phase ambiguities can be resolved to integers and an RMS of the K-band ranging system residuals of better than 0.7 mm can

be achieved, even though the orbital maneuver was performed on the spacecraft. Furthermore, the actual maneuver performance derived from the POD and PBD results provides rigorous feedback on the thruster system, which is not only beneficial for current maneuver assessment but also for future maneuver plans.

**Keywords** Maneuver · Precise orbit determination · Precise baseline determination · LEOs · GPS

## Introduction

Formation-flying low earth orbiters (LEOs) have been successfully used in earth remote sensing in the last few decades (Tapley and Reigber 2001; Krieger et al. 2007; D'Amico et al. 2013). Precise orbit determination (POD) and precise baseline determination (PBD) for LEOs are extremely important for high-accuracy applications. The use of GPS tracking data and reduced-dynamic technique (Wu et al. 1991) have allowed single-satellite POD of some LEOs to reach the centimeter level, such as CHAMP (Visser and van den Ijssel 2003), Jason-1 (Haines et al. 2004), GRACE (Jäggi et al. 2007), Jason-2 (Zelensky et al. 2010) and GOCE (Bock et al. 2014). The precision of inter-satellite PBD can even reach the millimeter level, such is the case for GRACE (Kroes et al. 2005) and TanDEM-X (Jäggi et al. 2012) formations.

Due to the effects of atmospheric drag, non-central gravitational forces or particular mission requirements, it is almost inevitable for LEOs to execute orbital maneuvers during their lifetimes. For example, to maintain a formation-flying configuration of  $220 \pm 50$  km separation in the along-track direction, formation-keeping maneuvers are performed 2–4 times per year for the GRACE mission

✉ Bing Ju  
supice@mit.edu; juice.nudt@gmail.com

<sup>1</sup> College of Science, National University of Defense Technology, Changsha 410073, China

<sup>2</sup> Department of Earth, Atmospheric, and Planetary Science, Massachusetts Institute of Technology, Cambridge, MA 02139, USA

<sup>3</sup> German Space Operations Center, Deutsches Zentrum für Luft- und Raumfahrt, 82230 Weßling, Germany

(Yoon et al. 2006). In addition, a leader/trailer swap maneuver which includes three sequential maneuvers was executed between December 2005 and January 2006 to balance the surface erosion of the K-band ranging (KBR) radars on both GRACE satellites (Montenbruck et al. 2006). Such swap maneuvers are now performed routinely about once every 6 months starting in June 2014. A more extreme example is the first spaceborne bistatic interferometry SAR mission TanDEM-X (Krieger et al. 2007), which consists of two almost identical satellites, i.e., TerraSAR-X (TSX) and TanDEM-X (TDX). In order to keep the TSX satellite flying in the predefined trajectory, orbit-keeping maneuvers need to be executed about once per week. These maneuvers must be replicated by the TDX satellite synchronously to avoid breaking up of the formation. Additional formation-keeping maneuvers must be performed on the TDX satellite twice per day to maintain a helix flying configuration (Jäggi et al. 2012). Similar and even more frequent maneuvers arise in the Prototype Research Instruments and Space Mission technology Advancement (PRISMA) mission, which is a Swedish-led autonomous formation-flying experiment (Gill et al. 2007). Coping with such frequent maneuvers, e.g., more than 20 maneuvers per day during a certain phase, is a key issue for both absolute and relative navigation for PRISMA formation (D'Amico et al. 2012, 2013).

Therefore, to avoid discontinuities and to connect pre- and post-maneuver arcs with a minimal set of parameters, routine orbit determination software should have the capability to simultaneously handle single and multiple maneuvers during one processing arc. For the EPOS and the BERNESE software packages used at the Germany Research Center for Geosciences (GFZ) and the Astronomical Institute of the University of Bern (AIUB), respectively, maneuvers are modeled as a series of velocity impulses at predefined epochs based on the execution time of each maneuver. These instantaneous velocity changes are estimated along with other parameters, e.g., dynamic parameters, pseudo-stochastic parameters, ambiguity parameters, in the least squares adjustment in both POD processing and PBD processing (Moon et al. 2012; Jäggi et al. 2012). For the GHOST software package used at the German Space Operations Center (DLR), maneuvers are treated as constant thrusts over specified intervals according to the burn start time and duration. In the POD processing, these parameters are estimated by reorganizing the interval of piecewise constant empirical accelerations around each maneuver in a batch least squares adjustment (Yoon et al. 2006, 2009). In the subsequent PBD processing, the POD result is used as an a priori trajectory and the remaining deficiencies between the estimated and real maneuvers are further compensated by including

supplementary process noise in the extended Kalman filter (EKF) (Montenbruck et al. 2011).

Maneuver calibration is an essential task for orbit control of LEOs (Yoon et al. 2006). A precise maneuver calibration is beneficial for both current maneuver assessment and future maneuver plans. While the actual maneuver performance compared with the planned one can be deduced from the in-flight telemetry data, the GPS tracking data collected onboard provides an alternative approach to perform maneuver calibration simultaneously with orbit determination processing. Since each maneuver is modeled as an instantaneous velocity change at a certain epoch, the EPOS and the BERNESE software will not provide accurate information of maneuver calibration for those maneuvers with long duration. The GHOST software only provides the information of maneuver calibration in POD but does not in PBD, because the estimation of maneuver parameters is beyond the scope of the EKF algorithm.

We implement a different maneuver handling approach in the software package of NUDTTK, which is used at the National University of Defense Technology (NDT) for precise orbit determination of LEOs. Our approach does not only provide continuous orbit and baseline solutions as accurate as those of a maneuver-free day, but also provides extra maneuver calibration information in both POD and PBD. In next section, we describe the reduced-dynamic model as well as the maneuver parameterization and estimation strategy used in our approach; especially, we propose a mixed integration strategy that employs both multistep and single-step methods to connect pre- and post-maneuver arcs. In subsequent sections, we demonstrate an application of the technique to GRACE single-satellite POD and inter-satellite PBD. The NUDTTK application is not limited to the GRACE mission, and it is also applicable to other LEO missions such as TanDEM-X and PRISMA.

## Processing methodology

Kinematic orbit determination is not affected by orbital maneuvers; it is, however, sensitive to observing geometry, noise and data outage, which limit its application in high-accuracy situations (Montenbruck et al. 2005). Reduced-dynamic orbit determination (Wu et al. 1991), which combines both dynamic constraints and the GPS observations, is preferred for generating continuous and precise orbital products for LEOs. Since each maneuver is generally accomplished by a short-term thrust onboard, it is necessary for this extra force to be modeled and estimated in such an orbit determination scheme.

## Reduced-dynamic orbit determination

The motion of a single LEO in the inertial frame can be described by the following deterministic differential equation,

$$\ddot{\mathbf{r}} = \mathbf{f}(t, \mathbf{r}, \dot{\mathbf{r}}, q_1, q_2, \dots, q_n) \quad (1)$$

where  $\mathbf{r}$  is the geocentric position vector of the spacecraft's center of mass,  $\dot{\mathbf{r}}$  and  $\ddot{\mathbf{r}}$  are the first and second time derivatives of  $\mathbf{r}$ , respectively, and  $q_1, q_2, \dots, q_n$  are unknown dynamic parameters to be estimated. The right-hand side function  $\mathbf{f}(\cdot)$  contains all gravitational and non-gravitational perturbations acting on the spacecraft, including potential maneuvers.

Given the initial conditions

$$\mathbf{r}_0 \triangleq \mathbf{r}(t_0); \quad \dot{\mathbf{r}}_0 \triangleq \dot{\mathbf{r}}(t_0) \quad (2)$$

the solution of (1) can be formally expressed as

$$\mathbf{r}(t) \triangleq \mathbf{r}(t, \mathbf{r}_0, \dot{\mathbf{r}}_0, q_1, q_2, \dots, q_n) \quad (3)$$

i.e., the trajectory  $\mathbf{r}(t)$  is a particular solution of (1) given the  $(n + 6)$  orbital parameters  $\mathbf{p} \triangleq (\mathbf{r}_0^T, \dot{\mathbf{r}}_0^T, q_1, q_2, \dots, q_n)$ .

If an alternative set of orbital parameters,  $\mathbf{p}^*$ , is used to solve (1) and  $\|\mathbf{p} - \mathbf{p}^*\|$  is assumed to be sufficiently small,  $\mathbf{r}(t)$  can be approximated by a first-order Taylor series, namely

$$\mathbf{r}(t) = \mathbf{r}^*(t) + \sum_{i=1}^{n+6} \mathbf{z}_i(t)(p_i - p_i^*) \quad (4)$$

where  $\mathbf{r}^*(t)$  is an a priori trajectory determined by  $\mathbf{p}^*$  and  $\mathbf{z}_i(t) \triangleq \partial \mathbf{r}^*(t) / \partial p_i$  is the solution of the so-called variational equation

$$\dot{\mathbf{z}}_i(t) = \frac{\partial \mathbf{f}}{\partial \mathbf{r}} \mathbf{z}_i(t) + \frac{\partial \mathbf{f}}{\partial \dot{\mathbf{r}}} \dot{\mathbf{z}}_i(t) + \frac{\partial \mathbf{f}}{\partial p_i} \quad (5)$$

which is derived by taking partial derivative of (1) with respect to  $p_i$ .

Given a set of observed quantities that can be related to the position vector of the satellite, we can write the generalized observation equation at epoch  $t_k$  as

$$y_k = h(\mathbf{r}(t_k)) + \varepsilon_k \quad (6)$$

where  $\varepsilon_k$  is the observation error of  $y_k$  with the expectation value of zero and  $h(\cdot)$  is the observation function, which is usually nonlinear.

By substituting (4) into (6) and then linearizing the system of equations, Eq. (6) can be rewritten as

$$y_k = h(\mathbf{r}^*(t_k)) + \sum_{i=1}^{n+6} (\nabla h(\mathbf{r}^*(t_k)))^T \mathbf{z}_i(t_k)(p_i - p_i^*) + \varepsilon_k \quad (7)$$

where  $\nabla h(\mathbf{r}^*(t_k))$  is the gradient of  $h(\cdot)$  at the position of  $\mathbf{r}^*(t_k)$ .

Therefore, given the appropriate initial values of  $\mathbf{p}^*$ , the orbital parameters  $\mathbf{p}$  can be estimated iteratively by solving the weighted least squares problem defined by (7). The orbital trajectories to be used in estimating parameters  $\mathbf{p}$  can be obtained by numerical integration of (1).

The method above outlines the principle of the dynamic orbit determination. As the force field acting on a low earth orbiting satellite is usually not known with sufficient accuracy, the reduced-dynamic approach (Wu et al. 1991) is widely used to compensate for deficiencies of the applied dynamical model. The key point of the reduced-dynamic method is to reduce the reliance on the a priori dynamical model and then to optimally combine the data strength and dynamical constraints. This can be realized by (a) adding process noise (typically suitable for Kalman filters) or (b) adding "pseudo-stochastic" or "empirical" parameters (typically suitable for batch least squares) to the a priori dynamical model and then solving the respective parameters from the GPS observations (Beutler et al. 2006).

We use the batch least squares strategy to perform the reduced-dynamic orbit determination. The piecewise linear empirical accelerations (Jäggi et al. 2006) are employed based on the use of a priori atmospheric drag and solar radiation pressure models. The detailed dynamical and measurement models used for POD and PBD of LEOs are summarized in Table 1.

It should be noted that the orbital parameters are always estimated together with non-orbital parameters such as ambiguities and receiver clock offsets. For the POD processing, the undifferenced (UD) ionospheric-free GPS measurement model is employed. Along with the orbital parameters, the receiver clock offsets and UD ionospheric-free ambiguities are estimated. For the PBD processing, the baseline solution is generated by a relative orbit determination procedure, which is based on the double-difference (DD) ionospheric-free GPS measurement model. The orbit of one satellite is kept fixed to its POD result, while the orbital parameters of the other satellite are estimated together with the DD ambiguities, which are resolved to their integer values by using the least squares ambiguity decorrelation adjustment (LAMBDA) algorithm (Teunissen 1995). Since the receiver clock offsets are eliminated in the DD model, they do not need to be estimated in the PBD processing.

## Maneuver thrust modeling

For orbit keeping of LEOs, the mass change during each maneuver can be ignored. Assuming a constant propellant mass-flow rate, the constant thrust model is usually sufficient to describe a maneuver in the body-fixed reference frame. On the other hand, in most cases the spacecraft will

**Table 1** Dynamical and measurement models employed in the NUDTTK software for GRACE POD and PBD

Item	Description
Gravitational forces	Earth gravity (GGM02C, $120 \times 120$ ); solid-earth, pole and ocean tides (IERS1996, CSR4.0); luni-solar-planetary gravity (DE405)
Non-gravitational forces	Atmospheric drag, Jacchia-Gill 71 density model, Cd is estimated per 24 h; solar radiation pressure (conical earth shadow), Canon-ball model, Cr is estimated per 24 h; empirical forces, piecewise linear model in R (tight constraint), T and N directions (no constraint) with subinterval length of 15 min; maneuver forces, constant thrust model for each maneuver in R, T and N directions over a predefined thrust interval
Reference frames	ITRF2005/IGS05 reference frame; IERS2003 reference frame transformations; CODE final ERPs
Measurement models	UD and DD ionospheric-free GPS code and phase observations (weighted) with 10 s sampling for POD and PBD, respectively; CODE final GPS orbits and 30 s clock offsets; igs05.atx PCO and PCVs corrections for GPS transmitter antennas; constant PCO and PCVs (estimated by NUDTTK) corrections for spaceborne receiver antennas
Estimator and integrator	Batch least squares estimator; an 11th-order Adams–Cowell integrator with 10 s step-size for normal and an eighth-order Runge–Kutta integrator for initializing the multistep integrator and connecting pre- and post-maneuver arcs

maintain a constant orientation with respect to the orbital frame during the period of maneuver (Montenbruck and Gill 2000). In our approach, each maneuver is treated as constant accelerations in radial (R), tangential (T) and normal (N) directions over a predefined time interval according to the burn time. Multiple maneuvers during one processing arc will be modeled and estimated simultaneously, as shown in Fig. 1. The burn timing information can usually be obtained from the in-flight telemetry data.

The maneuver accelerations in our dynamical model can be expressed as

$$\mathbf{a}_{\text{man}} = \sum_{i=1}^k (\alpha_{\text{R}}^i \mathbf{e}_{\text{R}}^i + \alpha_{\text{T}}^i \mathbf{e}_{\text{T}}^i + \alpha_{\text{N}}^i \mathbf{e}_{\text{N}}^i) \xi(t, t_s^i, t_e^i) \quad (8)$$

where  $\alpha_{\text{R}}^i$ ,  $\alpha_{\text{T}}^i$  and  $\alpha_{\text{N}}^i$  are maneuver parameters to be determined in the batch least squares adjustments,  $\xi(t, t_s^i, t_e^i)$  is equal to 1 for  $t \in [t_s^i, t_e^i)$ , otherwise equal to 0, where  $t_s^i$  and  $t_e^i$  are the known burn start and end times. The

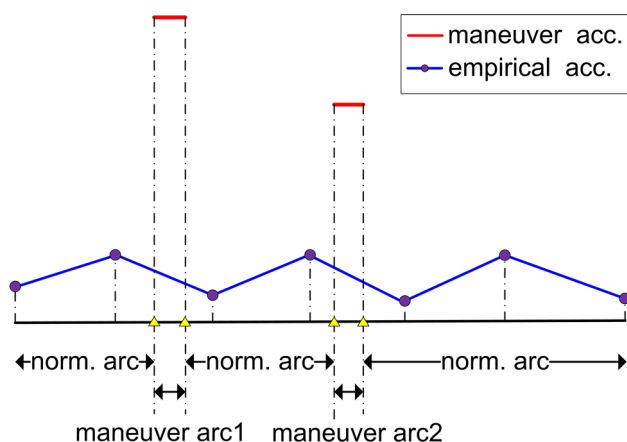


**Fig. 1** Sketch of maneuver accelerations together with piecewise linear empirical accelerations

symbols  $\mathbf{e}_{\text{R}}^i$ ,  $\mathbf{e}_{\text{T}}^i$  and  $\mathbf{e}_{\text{N}}^i$  denote the unit vectors of the R, T and N directions with respect to each specified maneuver.

The corresponding variational equation with respect to the specified maneuver parameter  $\alpha$  and the initial conditions are given as follows

$$\begin{cases} \dot{\mathbf{z}}_{\alpha}(t) = \frac{\partial \mathbf{f}}{\partial \mathbf{r}} \mathbf{z}_{\alpha}(t) + \frac{\partial \mathbf{f}}{\partial \mathbf{r}} \dot{\mathbf{z}}_{\alpha}(t) + \mathbf{e}^i \xi(t, t_s^i, t_e^i) \\ \mathbf{z}_{\alpha}(t_0) = \mathbf{0}; \quad \dot{\mathbf{z}}_{\alpha}(t_0) = \mathbf{0} \end{cases} \quad (9)$$

For  $t_0 \leq t < t_s^i$ , Eq. (9) is equivalent to a linear and homogeneous differential equation

$$\dot{\mathbf{z}}_{\alpha}(t) = \frac{\partial \mathbf{f}}{\partial \mathbf{r}} \mathbf{z}_{\alpha}(t) + \frac{\partial \mathbf{f}}{\partial \mathbf{r}} \dot{\mathbf{z}}_{\alpha}(t) \quad (10)$$

with zero initial conditions  $\mathbf{z}_{\alpha}(t_0) = \mathbf{0}$  and  $\dot{\mathbf{z}}_{\alpha}(t_0) = \mathbf{0}$ . Obviously, the solution  $\mathbf{z}_{\alpha}(t)$  will always be zero during this period. This means according to (7) that the measurements observed before epoch  $t_s^i$  will not make any contribution to the estimation of  $\alpha$ .

For  $t_s^i \leq t < t_e^i$ , Eq. (9) is equivalent to the following linear and inhomogeneous differential equation

$$\dot{\mathbf{z}}_{\alpha}(t) = \frac{\partial \mathbf{f}}{\partial \mathbf{r}} \mathbf{z}_{\alpha}(t) + \frac{\partial \mathbf{f}}{\partial \mathbf{r}} \dot{\mathbf{z}}_{\alpha}(t) + \mathbf{e}^i \quad (11)$$

with zero initial conditions  $\mathbf{z}_{\alpha}(t_s^i) = \mathbf{0}$  and  $\dot{\mathbf{z}}_{\alpha}(t_s^i) = \mathbf{0}$ . During this period, the solution  $\mathbf{z}_{\alpha}(t)$  is no longer kept to zero. Since a thrust is performed on the spacecraft, the trajectory  $\mathbf{r}(t)$  will be changed after epoch  $t_s$  and the accumulative influence will depend on the actual burn time. The solution of (11) is crucial to the estimation of  $\alpha$ , although the duration may be very short compared with the orbital period.

For  $t \geq t_e^i$ , Eq. (9) is equivalent to (10) but with nonzero initial conditions  $\mathbf{z}_{\alpha}(t_e^i) \neq \mathbf{0}$  and  $\dot{\mathbf{z}}_{\alpha}(t_e^i) \neq \mathbf{0}$ . The solution  $\mathbf{z}_{\alpha}(t)$  will not be equal to zero during this period, and the measurements obtained after epoch  $t_e^i$  will contribute to the estimation of  $\alpha$ .



In summary, the measurements observed after the start of a maneuver until the end of the processing arc all contribute to the estimation of the specified parameter  $\alpha$ . The maneuver parameters can be estimated even though there is no measurement during the period of the thrust. In practice, the difficulty lies in using a numerical integration method that will obtain a sufficiently accurate solution of the variational Eq. (9). Since the maneuver thrust often has a short duration and large magnitude, it is likely that poor numerical integration during maneuver and post-maneuver arcs will lead to an unreliable estimation of the thrust.

**Numerical integration around maneuver**

Multistep numerical integration methods are widely used in orbit determination processing, as they are more efficient than single-step methods (Montenbruck and Gill 2000). Because of the small orbital eccentricities for most of LEOs, an 11th-order Adams–Cowell (AC) method (Huang and Zhou 1993) with fixed step-size is employed in the NUDTTK software. In normal circumstances, it has been proved to be accurate and efficient for POD and PBD of LEOs (Gu and Yi 2011; Tu et al. 2012; Liu et al. 2014). In the case of maneuvers, however, the additional thrust accelerations will bring new challenges to the traditional AC integrator. As illustrated in Fig. 2, the deficiencies of the AC integrator with fixed step-size are presented in three typical cases.

**Case 1** The maneuver, whose duration is shorter than the step-size of the AC integrator, is performed between two adjacent epochs. In this situation, the maneuver parameters cannot be estimated. The numerical solution of (9) will always be zero, which leads to a singular normal matrix in the least squares adjustment.

**Case 2** The maneuver duration is as long as the step-size of the AC integrator, and there is only a single epoch in the thrust interval. In this situation, since the numerical solution of (9) is not equal to zero from epoch  $t_{k+2}$ , the maneuver parameters can be estimated when the traditional AC integrator is employed. However, due to the limited temporal resolution, bias between real thrust interval and actual compensated interval will lead to a mismatched error in orbit solution.

**Case 3** The maneuver duration is about three times as long as the step-size of the AC integrator. Since there is at least one epoch in the thrust interval, the maneuver parameters can be estimated analogously to Case 2. However, the main drawback is that the actual compensated thrust interval is only twice as long as the step-size, which also leads to a mismatched error.

The deficiencies demonstrated above can be partly mitigated by shortening the step-size of the traditional AC integrator. However, the smaller the step-size, the more computation cost and round-off errors will be incurred. Also the discontinuities caused by maneuver thrusts in the field of accelerations will lead to significant accuracy degradation for the multistep numerical integration method (Montenbruck and Gill 2000).

In light of these problems, we propose a modified AC integrator that jointly utilizes the multistep and single-step method around each maneuver. The output epochs of the modified integrator are kept the same as the traditional AC integrator, but a single-step integrator is activated when the current output epoch is going to enter, pass and leave a thrust interval. The principle of the proposed numerical integration is shown in Fig. 3. In order to meet the accuracy requirements, we use the eighth-order Runge–Kutta formulation of the DOPRI8 integrator (Prince and Dormand 1981) both during maneuvers and to restart the AC

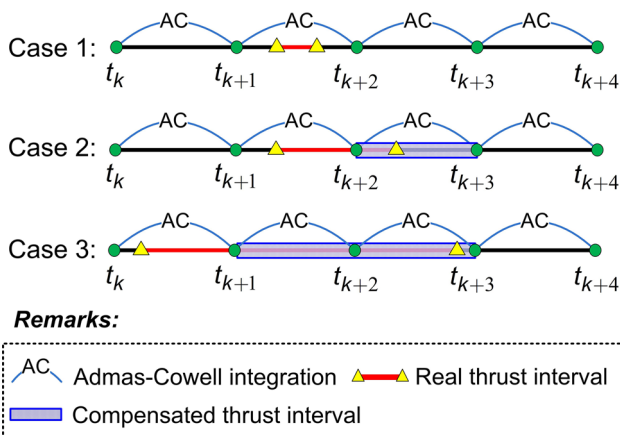


**Fig. 2** Deficiencies of the traditional AC integrator when dealing with an orbital maneuver

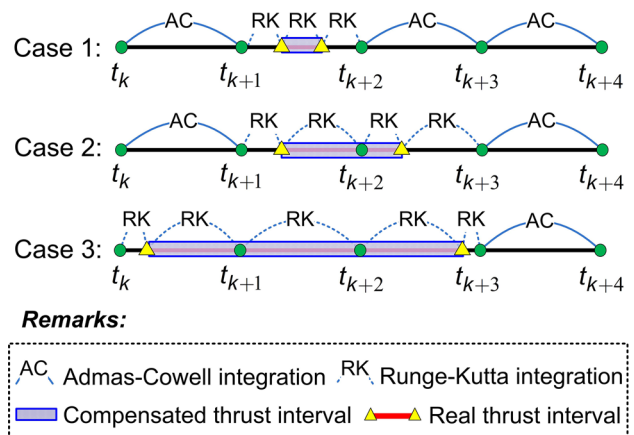


**Fig. 3** Strategy of the modified AC integrator around orbital maneuver

integrator after each maneuver. As the single-step integrator improves temporal resolution of the integration around the maneuver, the modified integrator will make the compensated thrust interval coincide with the real one.

## POD results

In order to evaluate the performance of maneuver handling for POD, we use ten one-day data sets from the GRACE mission. The maneuver information of each selected date is summarized in Table 2. Some additional explanations about these maneuvers are: (1) No maneuvers occurred on GRACE-A on these selected dates. Since the GRACE-A satellite was placed in the safe mode at the very beginning of the mission, all the subsequent maneuvers were performed on the GRACE-B satellite (Yoon et al. 2006). (2) The burn timing information is obtained from onboard telemetry data with an uncertainty of 1–2 s. (3) Each maneuver was executed by two 40 mN orbital trim thrusters, which can be operated individually or in pairs (Yoon et al. 2006). As shown in the far right column in Table 2, most of the selected maneuvers were only executed by one thruster, except on the three dates of June 7, 2005, December 12, 2005, and January 11, 2006. (4) Almost all the maneuvers are performed as thrusts in-flight or anti-flight directions, except for the one on April 6, 2005. As a preparation for the coming switch maneuver, this latter maneuver is an inclination maneuver that is designed to induce a drift in the normal direction (Yoon et al. 2006).

## Orbit determination residuals

In Fig. 4, the performance of maneuver handling is shown by examining the ionospheric-free phase residuals. When there is no maneuver modeling, the residuals are very large in vicinity of the maneuver, because the mis-modeled thrust cannot be sufficiently compensated by the empirical

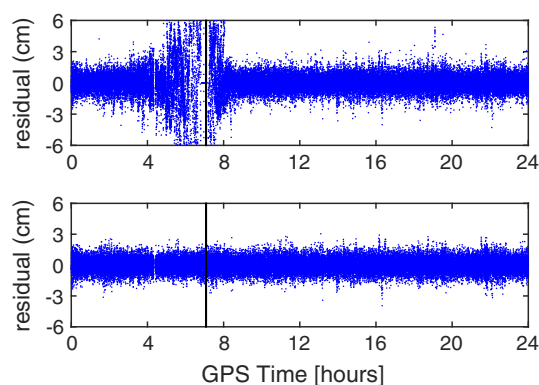


**Fig. 4** Ionospheric-free phase residuals without maneuver modeling (*top*) versus those with maneuver modeling (*bottom*) for GRACE-B on July 4, 2012. The *vertical bar* indicates the center of burn time. Residuals exceeding  $\pm 6$  cm around the maneuver are not shown in the *top panel*

accelerations. When maneuver modeling is taken into account, the large deviations are almost eliminated. The RMS of the residuals is decreased from 4.4 cm to 0.6 cm.

In Table 3, the RMS of the ionospheric-free phase residuals of the GRACE-B satellite is given for each selected date. With maneuver modeling, the orbit determination residuals are improved distinctly. The improvement is especially large for the long-duration maneuver on December 12, 2005, where the residual RMS was improved from 53.3 to 0.6 cm. In addition, as the twin GRACE satellites are equipped with the same GPS receivers and in the analogous in-flight situations, the RMS of the ionospheric-free phase residuals of the GRACE-A satellite is given as a reference. The orbit determination residuals of the maneuvering GRACE-B satellite are of the same size as those of the maneuver-free GRACE-A satellite indicating

**Table 2** Maneuver information of GRACE-B on selected dates

Maneuver day	Date	Start time (GPST)	Duration (s)	No. of thruster
1	2004-09-29	13:52:46	64.3	1
2	2005-04-06	05:49:20	129.6	1
3	2005-06-07	05:45:10	24.5	2
4	2005-12-12	17:05:44	611.2	2
5	2006-01-11	12:53:04	53.1	2
6	2009-07-28	13:10:13	90.8	1
7	2010-05-19	04:44:45	102.0	1
8	2011-02-08	08:06:53	118.4	1
9	2011-08-17	06:36:59	121.4	1
10	2012-07-04	07:03:38	117.4	1

**Table 3** RMS (cm) of the ionospheric-free phase residuals of GRACE-A (maneuver free), GRACE-B without maneuver modeling and GRACE-B with maneuver modeling

Date	GRACE-A	GRACE-B	
	No maneuver	Without maneuver modeling	With maneuver modeling
2004-09-29	0.6	2.8	0.6
2005-04-06	0.6	9.2	0.6
2005-06-07	0.6	2.2	0.6
2005-12-12	0.6	53.3	0.6
2006-01-11	0.6	5.9	0.6
2009-07-28	0.6	4.8	0.6
2010-05-19	0.6	5.5	0.6
2011-02-08	0.6	5.8	0.7
2011-08-17	1.1	4.4	1.0
2012-07-04	0.7	4.4	0.6

that our maneuver accommodated orbits fit the GPS observations well.

**External orbit comparisons**

The GRACE orbit solutions generated by the Jet Propulsion Laboratory (JPL) and DLR are employed as external comparisons. For the JPL orbit (Bertiger et al. 2010), no attempt is made to accommodate orbital maneuver but only to break up the processing arc into pre- and post-maneuver arcs. For the DLR orbit (Montenbruck et al. 2005), maneuver is taken into account in the POD processing as described in the introduction.

In Fig. 5, the differences among the NDT, DLR and JPL orbits in T direction are illustrated for the GRACE-B satellite on July 4, 2012. The significant fluctuation of the JPL orbit can be observed in vicinity of the maneuver when compared with the NDT and DLR orbits. However, the differences between the NDT and DLR orbits are quite small during this period. These comparisons indicate that the maneuver accommodated NDT and DLR orbits perform better than the JPL orbit in relation to orbital continuity.

In Fig. 6, the RMS of the differences between the NDT and DLR orbits is shown for each maneuver day. The mean RMS for GRACE-B satellite in R, T and N directions is 1.3, 1.5 and 1.5 cm, respectively. The mean 3D RMS of the differences is 2.5 cm. These results are consistent with the precision obtained for maneuver-free GRACE-A satellite, which is on average of 2.6 cm (3D RMS) on these selected dates.

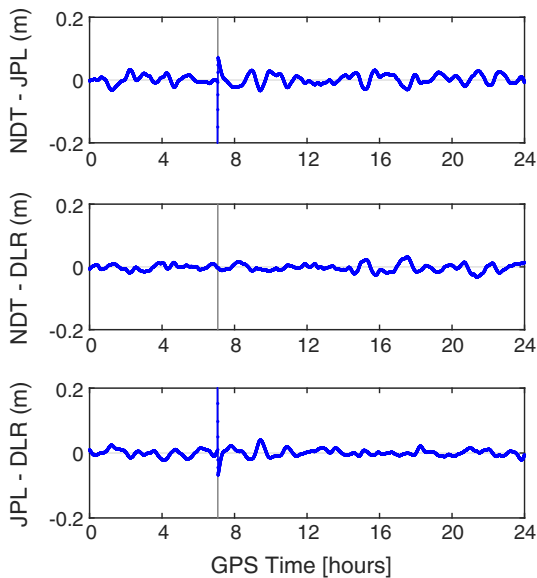


**Fig. 5** Differences among NDT, DLR and JPL orbits in T direction for GRACE-B on July 4, 2012. The vertical bar indicates the center of burn time

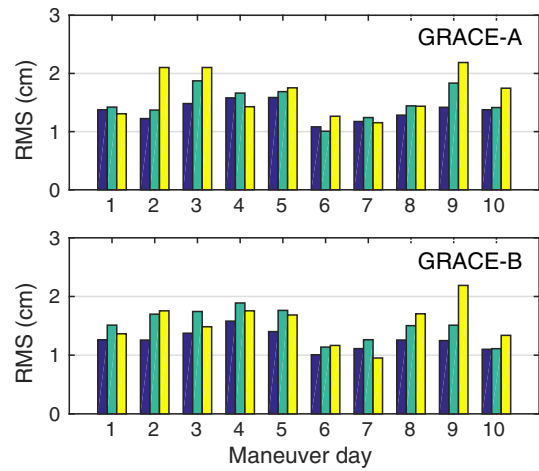


**Fig. 6** RMS of the differences between the NDT and DLR orbits for GRACE-A (top) and GRACE-B (bottom). The left, middle and right bars indicate the RMS in R, T and N directions, respectively

**Maneuver assessment by POD**

Maneuver handling is not only important for the routine POD processing, but also for current maneuver calibration and further maneuver plans. Each maneuver performance derived from the POD result can be employed as an evaluation for the thruster system onboard.

The maneuver on a GRACE satellite is usually planned in the form of a  $\delta v$  in the body-fixed frame. As the spacecraft maintains a constant orientation with respect to the RTN frame during the thrust phase, the estimated maneuver acceleration  $\mathbf{a}_{man}$  can be simply converted to the corresponding velocity change by  $\delta v = \|\mathbf{a}_{man}\Delta t\|$  using the knowledge of burn time  $\Delta t$ . The maneuver acceleration estimated by POD together with the corresponding velocity change is given in Table 4.

As shown in Table 4, the magnitude of R component of each maneuver acceleration is very small (about  $10^{-7}$ – $10^{-6}$   $m/s^2$ ) compared with the other two components. This small magnitude indicates that the pitch attitude of the spacecraft is well maintained during the period of thrust, which is important for executing the planned maneuver. The largest thrust component appears in T direction for all of these maneuvers, except for the one on April 6, 2005. According to the maneuver information given earlier, the thrust performed on April 6, 2005, with the largest component in N direction, can be confirmed as an inclination maneuver rather than a tangential maneuver. The maneuver accelerations in T direction on June 7, 2005, December 12, 2005, and January 11, 2006, which were executed by the two orbital trim thrusters simultaneously, are indeed about twice as large as other tangential maneuvers performed by only one thruster.



**Table 4** Maneuver acceleration and corresponding  $\delta v$  derived by POD of GRACE-B

Date	$\alpha_R$ ( $10^{-7}$ m/s <sup>2</sup> )	$\alpha_T$ ( $10^{-5}$ m/s <sup>2</sup> )	$\alpha_N$ ( $10^{-5}$ m/s <sup>2</sup> )	$\delta v$ (mm/s)
2004-09-29	5.81	7.48	1.18	4.87
2005-04-06	4.79	1.34	8.30	10.89
2005-06-07	-1.03	16.20	-0.21	3.97
2005-12-12	-7.87	16.29	-0.15	99.55
2006-01-11	-4.03	16.25	-0.16	8.62
2009-07-28	-6.44	-7.80	-1.16	7.16
2010-05-19	-2.83	-7.75	-1.17	7.99
2011-02-08	-6.83	-7.94	-1.20	9.51
2011-08-17	3.94	-7.98	-1.24	9.81
2012-07-04	-3.27	-8.03	-1.24	9.53

Secondly, the reason there is a non-ignorable N component for the tangential maneuver using one thruster onboard is due to the geometry configuration of the two orbital trim thrusters. These two thrusters are located symmetrically on the  $x$ - $y$  plane of the body-fixed reference frame of the satellite, which introduces an angle offset of about  $9.1^\circ$  between each thrust vector and the  $x$ -axis (Yoon et al. 2006). Therefore, under the assumption of a normal attitude during the period of maneuver, the thrust executed by only one orbital trim thruster will lead to an N component with the size of about 16 % of the T component. This can also be further confirmed by the results of those three maneuvers using both of the two thrusters, whose N component is clearly reduced by employing the two symmetrical thrusters.

The relative error of the estimated  $\delta v$  with respect to the planned one is given in Fig. 7. In addition, the  $\delta v$  derived from onboard telemetry (Yoon et al. 2006) is employed as an independent validation. It is not possible to decide which type of calibration is more accurate without additional information, but the maneuver performance derived from GPS-based POD and onboard telemetry are consistent. The relative error of the executed maneuver for GRACE mission is  $<5\%$  with respect to the planned one.

## PBD results

Precise baseline determination is another essential mission for formation-flying LEOs. Using the DD GPS observation models, we are not only able to largely reduce the estimated parameters by eliminating receiver clock offsets, but also to employ the integer property of the DD ambiguities to fully exploit the high-accuracy carrier phase measurements. In this section, we will mainly focus on the performance of maneuver handling for inter-satellite baseline determination. The GRACE data sets given in Table 2 will be used in the PBD processing.

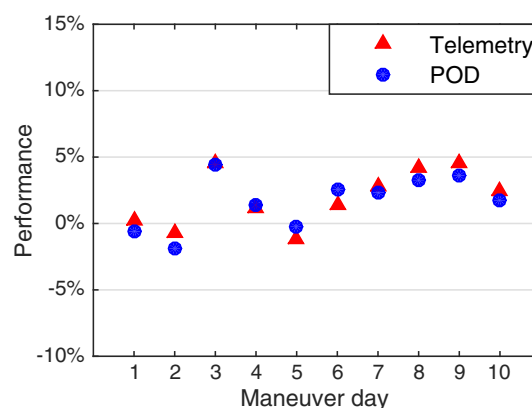


**Fig. 7** Maneuver performance derived from POD and onboard telemetry of GRACE-B

## Rate of the DD ambiguities resolution to integer values

In the PBD processing, we use the well-known wide-lane and narrow-lane strategy to fix the integer DD ambiguities. The carrier phase measurements will be transformed to high-accuracy constraints of the relative distances only if both of the wide-lane DD ambiguities and the narrow-lane DD ambiguities are fixed to the integer values correctly.

The wide-lane DD ambiguities are formed by the Hatch–Melbourne–Wübbena (HMW) linear combination (Hatch 1982) of the dual-frequency GPS observations and are then resolved to integers using the LAMBDA algorithm (Teunissen 1995). The fixing rate of the wide-lane DD ambiguities is not dependent on dynamic models because the HMW linear combination removes the geometry as well as the ionospheric contributions from the number of cycles between L1 and L2. However, the narrow-lane DD ambiguities are first estimated as float values along with other dynamic parameters and then taken with the accompanying covariance to perform the integer least squares estimation. Thus, the fixing rate of the narrow-lane

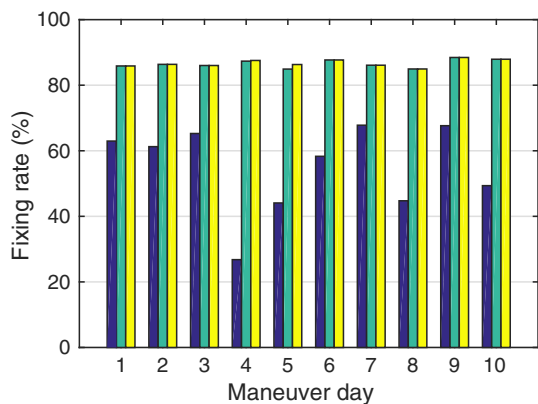


**Fig. 8** Percentage of the fixed ambiguities for both wide-lane and narrow-lane DD ambiguities. The *left* and *middle* bars indicate the fixing rate of narrow-lane DD ambiguities without and with maneuver modeling, respectively; the *right* bar indicates the fixing rate of wide-lane DD ambiguities

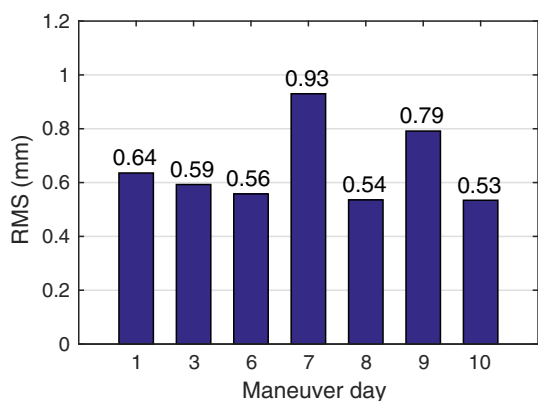


**Fig. 9** RMS of the KBR residuals for PBD results with maneuver modeling

DD ambiguities depends on the precision of the prior float-value solutions, which are strongly related to the dynamic models. If the orbital maneuver cannot be handled properly, the narrow-lane DD ambiguities will not be fixed correctly either.

In Fig. 8, we show for ten maneuver events the percentage of wide-lane ambiguities resolved and the percentages of narrow-lane ambiguities resolved with and without maneuver modeling. As the validation criterion, we use the ratio of the squared norms of the best and second best integer DD ambiguity residuals, with the typical threshold of 3 (Leick et al. 2015). On average, 87 % of the wide-lane DD ambiguities can be resolved to integer values. The narrow-lane DD ambiguities will be resolved only if the corresponding wide-lane DD ambiguities were resolved successfully. When there is no maneuver modeling, the float-value solutions of the narrow-lane DD ambiguities will be seriously affected by the mis-modeled

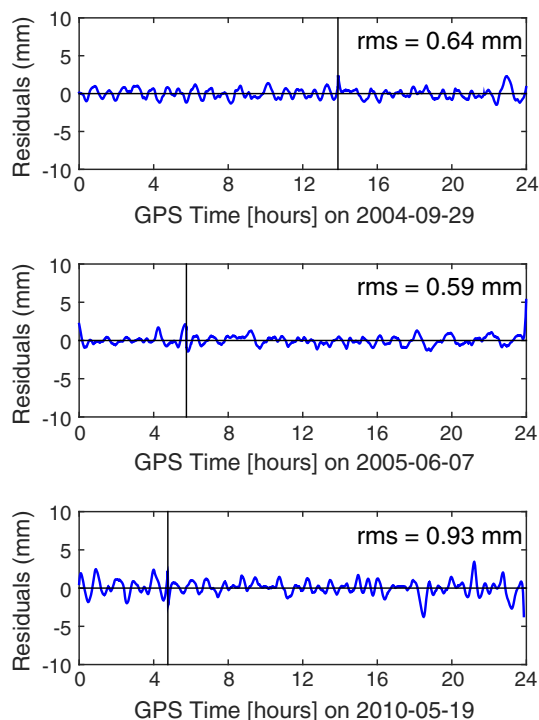


**Fig. 10** KBR residuals for the PBD results on September 29, 2004, June 7, 2005, and May 19, 2010. The *vertical* bars indicate the center of burn time

thrust which leads to a very low fixing rate (55 % on average). The worst case appears on December 12, 2005, which has the longest thrust duration and the fixing rate of the narrow-lane DD ambiguities is only 27 %. When maneuver modeling is taken into account, almost all of the narrow-lane ambiguities corresponding to resolved wide lanes are now resolved. The result is comparable with PBD results for maneuver-free days.

### KBR residuals

The KBR system is the main instrument on both GRACE satellites used to derive the variation of the earth's gravity field. It employs dual one-way ranging mode to track distance changes between the two satellites with a precision of about ten micrometers (Kroes et al. 2005). These accurate and independent observations can be used to validate the GPS-based PBD results for the GRACE mission. However, sometimes the KBR link is interrupted for a few hours, because a prior yaw maneuver is required for some particular orbital maneuvers. For the inclination maneuver on April 6, 2004, approximately 2 h of the KBR data were lost, and for the two swap maneuvers on December 12, 2005, and January 11, 2006, about 6 h of the KBR data were lost. In the following analysis, these 3 days will be excluded due to large gap of the KBR data in vicinity of the maneuver.

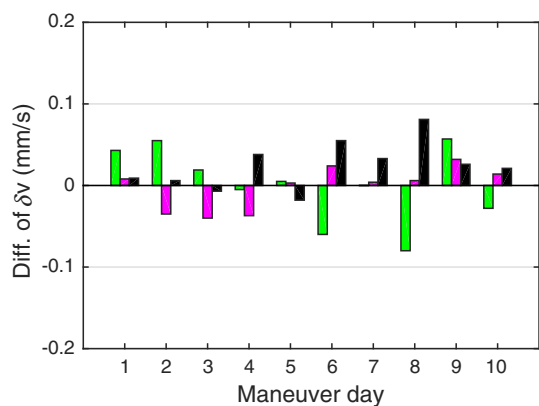


**Fig. 11** Difference of the estimated  $\delta v$  between POD and PBD in each axis. The *left, middle* and *right* bars indicate the difference in R, T and N directions, respectively

The RMS of the KBR residuals for each PBD result is given in Fig. 9. Due to appropriate handling of the maneuver thrust and high fixing rate of the DD ambiguities, the average RMS of the KBR residuals is 0.65 mm. In Fig. 10, the KBR residuals for PBD results on September 29, 2004, June 7, 2005, and May 19, 2010, are demonstrated, respectively. There is no large fluctuation around each maneuver, and the maximum deviation during this period is  $<5$  mm, comparable to those during other parts of the orbit. Millimeter-level baseline determination for the maneuvering GRACE-B satellite can still be achieved without the need to divide the processing arc into pre- and post-maneuver arcs.

### Maneuver assessment by PBD

The maneuver performance can also be derived from the relative orbit determination processing. In this section, we will have a discussion on maneuver calibration that can be obtained by the DD baseline determination.

Since common errors can be largely eliminated in the DD measurement model, the maneuver performance derived from PBD should be more accurate than that derived from single-satellite POD. However, as shown in Fig. 11, the difference of the estimated  $\delta v$  between POD and PBD is quite small. The relative error of the total velocity change is not more than 1%. In view of the tiny difference, the POD-based maneuver calibration is recommended with priority, because it is more widely used for both single and formation-flying LEOs. This preference is also sustained in the robustness of the majority of algorithms for POD. The “trust” on maneuver calibration from PBD is inherently dependent on the robustness of the PBD algorithm, which in turn is highly dependent on the robustness of the integer ambiguity resolution scheme.

### Conclusions

The maneuver handling for single-satellite POD and inter-satellite PBD of LEOs was studied in a reduced-dynamic scheme. In order to evaluate actual maneuver handling performance, the GRACE formation was used to validate our approach. With the proper thrust modeling and numerical integration strategy, the effects caused by orbital maneuver can be largely eliminated from the POD and PBD results.

The orbit determination residuals of the maneuvering GRACE-B satellite are at the same level as those of the maneuver-free GRACE-A satellite, which indicates that our maneuver accommodated orbit fits to the GPS observations well. An external orbit validation shows that the orbit obtained from our approach performs better than the JPL orbit in respect of continuity and matches the DLR orbit better than 3 cm (3D RMS). With maneuver modeling, 87% of DD phase ambiguities can be resolved, comparable to the rate for normal orbits. An RMS of the KBR validation of better than 0.7 mm can be obtained, which indicates that 1 mm baseline solution for the GRACE formation can be achieved even when there is an orbital maneuver was performed on the spacecraft.

In order to perform good mission planning, one has to also understand the performance of propulsion system on a spacecraft. Usually, thruster behaviors could not be predicted exactly from onboard telemetry data after so many maneuvers. The maneuver performance derived from GPS-based POD provides rigorous and independent feedback on the thruster system.

**Acknowledgments** This research was supported by the National Natural Science Foundation of China (Nos. 61370013 and 91438202). The authors would like to thank the Information Systems and Data Center (ISDC) and the German Space Operations Center (GSOC) for providing the science data and maneuver information of the GRACE mission. We also want to acknowledge Dr. Yoke Yoon for providing the information that helped the research and reviewing the paper. Last but not least, the comments and suggestions of the anonymous reviewers are greatly appreciated.

### References

- Bertiger W, Desai S, Haines B et al (2010) Single receiver phase ambiguity resolution with GPS data. *J Geod* 84(5):327–337. doi:[10.1007/s00190-010-0371-9](https://doi.org/10.1007/s00190-010-0371-9)
- Beutler G, Jäggi A, Hugentobler U, Mervart L (2006) Efficient satellite orbit modelling using pseudo-stochastic parameters. *J Geod* 80(7):353–372. doi:[10.1007/s00190-006-0072-6](https://doi.org/10.1007/s00190-006-0072-6)
- Bock H, Jäggi A, Beutler G, Meyer U (2014) GOCE: precise orbit determination for the entire mission. *J Geod* 88(11):1047–1060. doi:[10.1007/s00190-014-0742-8](https://doi.org/10.1007/s00190-014-0742-8)
- D’Amico S, Ardaens JS, Larsson R (2012) Spaceborne autonomous formation-flying experiment on the PRISMA mission. *J Guid Control Dyn* 35(3):834–850. doi:[10.2514/1.55638](https://doi.org/10.2514/1.55638)

- D'Amico S, Ardaens JS, Flobio SD (2013) Autonomous formation flying based on GPS-PRISMA flight results. *Acta Astronaut* 82(1):69–79. doi:[10.1016/j.actaastro.2012.04.033](https://doi.org/10.1016/j.actaastro.2012.04.033)
- Gill E, D'Amico S, Montenbruck O (2007) Autonomous formation flying for the PRISMA mission. *J Spacecr Rockets* 44(3): 671–681. doi:[10.2514/1.23015](https://doi.org/10.2514/1.23015)
- Gu DF, Yi DY (2011) Reduced dynamic orbit determination using differenced phase in adjacent epochs for spaceborne dual-frequency GPS. *Chin J Aeronaut* 24(6):789–796. doi:[10.1016/S1000-9361\(11\)60093-9](https://doi.org/10.1016/S1000-9361(11)60093-9)
- Haines H, Bar-Sever Y, Bertiger W, Desai S, Willis P (2004) One-centimeter orbit determination for Jason-1: new GPS-based strategies. *Mar Geod* 27:299–318. doi:[10.1080/01490410490465300](https://doi.org/10.1080/01490410490465300)
- Hatch R (1982) The synergism of GPS code and carrier measurements. In: *Proceedings of the third international symposium on satellite Doppler positioning at physical sciences laboratory of New Mexico State University*, vol 2, pp 1213–1231
- Huang TY, Zhou QL (1993) Adams–Cowell integrator with a first sum. *Chin Astron Astrophys* 17(2):205–213. doi:[10.1016/0275-1062\(93\)90071-V](https://doi.org/10.1016/0275-1062(93)90071-V)
- Jäggi A, Hugentobler U, Beutler G (2006) Pseudo-stochastic orbit modeling techniques for low-earth orbiters. *J Geod* 80(1):47–60. doi:[10.1007/s00190-006-0029-9](https://doi.org/10.1007/s00190-006-0029-9)
- Jäggi A, Hugentobler U, Bock H, Beutler G (2007) Precise orbit determination for GEACE using undifferenced or doubly differenced GPS data. *Adv Space Res* 39(10):1612–1619. doi:[10.1016/j.asr.2007.03.012](https://doi.org/10.1016/j.asr.2007.03.012)
- Jäggi A, Montenbruck O, Moon Y et al (2012) Inter-agency comparison of TanDEM-X baseline solutions. *Adv Space Res* 50(2):260–271. doi:[10.1016/j.asr.2012.03.027](https://doi.org/10.1016/j.asr.2012.03.027)
- Krieger G, Moreira A, Fiedler H et al (2007) TanDEM-X: a satellite formation for high-resolution SAR interferometry. *IEEE Trans Geosci Remote Sens* 45(11):3317–3341. doi:[10.1109/TGRS.2007.900693](https://doi.org/10.1109/TGRS.2007.900693)
- Kroes R, Montenbruck O, Bertiger W, Visser P (2005) Precise GRACE baseline determination using GPS. *GPS Solut* 9:21–31. doi:[10.1007/s10291-004-0123-5](https://doi.org/10.1007/s10291-004-0123-5)
- Leick A, Rapoport L, Tatarnikov D (2015) *GPS satellite surveying*, 4th edn. Wiley, New York
- Liu JH, Gu DF, Ju B et al (2014) Basic performance of BeiDou-2 navigation satellite system used in LEO satellites precise orbit determination. *Chin J Aeronaut* 27(5):1251–1258. doi:[10.1016/j.cja.2014.03.006](https://doi.org/10.1016/j.cja.2014.03.006)
- Montenbruck O, Gill E (2000) *Satellite orbits: models, methods and applications*. Springer, Berlin
- Montenbruck O, van Helleputte T, Kroes R, Gill E (2005) Reduced dynamic orbit determination using GPS code and carrier measurements. *Aerosp Sci Technol* 9(3):261–271. doi:[10.1016/j.ast.2005.01.003](https://doi.org/10.1016/j.ast.2005.01.003)
- Montenbruck O, Kirschnner M, D'Amico S, Bettadpur S (2006) E/I-vector separation for safe switching of the GRACE formation. *Aerosp Sci Technol* 10(7):628–635. doi:[10.1016/j.ast.2006.04.001](https://doi.org/10.1016/j.ast.2006.04.001)
- Montenbruck O, Wermuth M, Kahle R (2011) GPS based relative navigation for the TanDEM-X mission—first flight results. *Navigation* 58(4):293–304. doi:[10.1002/j.2161-4296.2011.tb02587.x](https://doi.org/10.1002/j.2161-4296.2011.tb02587.x)
- Moon Y, Koenig R, Wermuth M (2012) Operational precise baseline determination for TanDEM-X DEM processing. In: *Proceedings of IEEE international geoscience and remote sensing symposium at Munich*, July 22–27, pp 1633–1636. doi:[10.1109/IGARSS.2012.6351215](https://doi.org/10.1109/IGARSS.2012.6351215)
- Prince PJ, Dormand JR (1981) High order embedded Runge–Kutta formulae. *J Comp Appl Math* 7(1):67–75. doi:[10.1016/0771-050X\(81\)90010-3](https://doi.org/10.1016/0771-050X(81)90010-3)
- Tapley BD, Reigber C (2001) The GRACE mission: status and future plans. *EOS Trans AGU* 82(47), Fall Meet. Suppl. G41 C-02
- Teunissen PJG (1995) The least-squares ambiguity decorrelation adjustment: a method for fast GPS integer ambiguity estimation. *J Geod* 70(1–2):65–82. doi:[10.1007/BF00863419](https://doi.org/10.1007/BF00863419)
- Tu J, Gu DF, Wu Y, Yi DY (2012) Phase residual estimations for PCVs of spaceborne GPS receiver antenna and their impacts on precise orbit determination of GRACE satellites. *Chin J Aeronaut* 25(4):631–639. doi:[10.1016/S1000-9361\(11\)60428-7](https://doi.org/10.1016/S1000-9361(11)60428-7)
- Visser P, van den Ijssel J (2003) Aiming at a 1-cm orbit for low earth orbiters: reduced-dynamic and kinematic precise orbit determination. *Space Sci Rev* 108(1–2):27–36. doi:[10.1023/A:1026253328154](https://doi.org/10.1023/A:1026253328154)
- Wu SC, Yunck TP, Thornton CL (1991) Reduced-dynamic technique for precise orbit determination of low earth satellites. *J Guidance Control Dyn* 14(1):24–30. doi:[10.2514/3.20600](https://doi.org/10.2514/3.20600)
- Yoon YT, Montenbruck O, Kirschnner M (2006) Precise maneuver calibration for remote sensing satellites. In: *Proceedings of the 19th international symposium on space flight dynamics at Kanazawa*, June 4–11, pp 607–612
- Yoon YT, Eineder M, Yague-Martinez N, Montenbruck O (2009) TerraSAR-X precise trajectory estimation and quality assessment. *IEEE Trans Geosci Remote Sens* 47(6):1859–1868. doi:[10.1109/TGRS.2008.2006983](https://doi.org/10.1109/TGRS.2008.2006983)
- Zelensky NP, Lemoine FG, Ziebart M et al (2010) DORIS/SLR POD modeling improvements for Jason-1 and Jason-2. *Adv Space Res* 46(12):1541–1558. doi:[10.1016/j.asr.2010.05.008](https://doi.org/10.1016/j.asr.2010.05.008)



**Bing Ju** is a Ph.D. candidate in Applied Mathematics at the National University of Defense Technology in China. He received his B.S. and M.S. degrees from the National University of Defense Technology in 2009 and 2011, respectively. His current research activities are focus on multi-GNSS data processing and precise orbit determination for low earth orbiters.



**Defeng Gu** is an associate professor at the National University of Defense Technology in China. He received his B.S. and Ph.D. degrees from the National University of Defense Technology in 2003 and 2009, respectively. His research interests are modern statistical method and measurement data processing. His current research activities involve GNSS data processing and precise relative navigation for formation-flying LEOs.





**Thomas A. Herring** received his bachelor's and master's degrees in geodetic science from the University of Queensland in Australia in 1976 and 1978. His Ph.D. in geophysics, awarded in 1983, is from MIT. Professor Herring joined the MIT faculty in 1989. His research interests are in the development and applications of precise geodetic techniques to study deformation processes on all spatial and temporal scales.

Service and coordinates the performance of the MGEX Multi-GNSS Experiment.



**Zhengming Wang** is a professor at the National University of Defense Technology in China. He received his B.S. and M.S. degrees in Applied Mathematics and Ph.D. degree in System Engineering in 1982, 1986 and 1998, respectively. His current research activities comprise mathematical modeling in tracking data, experiment design and evaluation, remote sensing image processing and data fusion theory.



**Gerardo Allende-Alba** is a Ph.D. candidate at the Technische Universität München and the DLR's German Space Operations Center. In 2012, he received his M.S. degree in Earth-Oriented Space Science and Technology from the Technische Universität München and his B.S. degree in 2008 from the Instituto Politécnico Nacional in Mexico City. His current research activities are focused on precise relative navigation for dis-

tributed spacecraft in LEO.



**Oliver Montenbruck** is head of the GNSS Technology and Navigation Group at DLR's German Space Operations Center. His research activities comprise spaceborne GNSS receiver technology, autonomous navigation systems, spacecraft formation flying and precise orbit determination as well as new constellations and multi-GNSS processing. Oliver Montenbruck presently chairs the Multi-GNSS Working Group of the International GPS